

Mesoporous Structures

Phenyl Groups Result in the Highest Benzene Storage and Most Efficient Desulfurization in a Series of Isostructural Metal–Organic Frameworks

Wen-Wen He,^[a] Guang-Sheng Yang,^[a] Yu-Jia Tang,^[b] Shun-Li Li,^[b] Shu-Ran Zhang,^[a] Zhong-Min Su,^{*[a]} and Ya-Qian Lan^{*[a, b]}

Abstract: A series of isorecticular metal–organic frameworks (MOFs; **NENU-511–NENU-514**), which all have high surface areas and strong adsorption capacities, have been successfully constructed by using mixed ligands. **NENU-513** has the highest benzene capacity of 1687 mg g⁻¹ at 298 K, which ranks as the top MOF material among those reported up to now. This **NENU** series has been used for adsorptive desulfurization because of its permanent porosity. The results

indicate that this series has a higher adsorptive efficiency in the removal of organosulfur compounds than other MOF materials, especially **NENU-511**, which has the highest adsorptive efficiency in the ambient atmosphere. This study proves that the design and synthesis of targeted MOFs with higher surface areas and with functional groups present is an efficient method to enhance benzene-storage capacity and the adsorption of organosulfur compounds.

Introduction

The release of harmful chemicals into our environment has been a sustained security concern along with the rapid development of the industrial world.^[1] The effective capture of these chemicals is of great significance, not only to the environment, but also to the people who are at risk for exposure to such materials.^[2] Benzene and its derivatives are one of the basic petrochemical feedstocks and can be applied in a variety of chemical industrial processes. However, as volatile and strongly carcinogenic chemicals, the release of such organic emissions will cause a lot of health issues, such as aplastic anemia or leukemia. Adsorption is an efficient way to solve this problem.^[3] Nowadays, filters are often composed of pure activated carbon or carbon materials with some simple modification. The current applications of activated carbon materials are limited because of the low selectivity toward some chemicals and the lack of control over the highly amorphous nature of the carbon network. Therefore, researchers are looking for new materials to adsorb benzene and other volatile toxic substances effectively.^[4] Metal–organic frameworks (MOF) have

emerged as a new class of porous crystalline organic–inorganic polymer, which have been at the forefront of the materials science field over the past few years.^[5] Owing to their properties of high porosity and tunable structural architectures, MOFs have become one of the most promising materials in the application of gas/vapor storage and separation.^[3a,6] In 2008, Yaghi and co-workers reported the good adsorption performance of MOF materials, for which an efficacy greater than the Calgon BPL activated carbon was demonstrated for the absorption of benzene molecules.^[2] Furthermore, their unique properties, such as tunable size and various modification of the ligand in the framework, will open new perspectives on the application of the storage of benzene and other toxic substances.^[7]

Meanwhile, the desulfurization of fuels is also an urgent issue worldwide because the sulfur compounds present in transportation fuels will not only result in the formation of acid rain, but these compounds also poison noble-metal catalysts used to reduce CO and NO_x emissions.^[8] The currently adopted industrial method is catalytic hydrodesulfurization (HDS), oxidative desulfurization (ODS), oxidation–extraction desulfurization (OEDS), bio-desulfurization (BDS), and so forth.^[9] But the high-temperature high-pressure catalytic process, high hydrogen consumption, and the low selectivity for refractory sulfur-containing compounds, such as dibenzothiophene and its derivatives, greatly restrict the application of these methods. Nowadays, adsorption has become a competitive alternative way to remove sulfur contaminants because the adsorbent can be regenerated and the whole process is much milder.^[5a,10] Recently, MOFs have been applied to the study of desulfurization due to the controllability of their structure.^[11] Matzger and co-workers and Jhung and co-workers have carried out a lot of

[a] Dr. W.-W. He, Dr. G.-S. Yang, Dr. S.-R. Zhang, Prof. Z.-M. Su, Prof. Y.-Q. Lan
Institute of Functional Material Chemistry
Faculty of Chemistry, Northeast Normal University
Changchun, 130024 Jilin (P.R. China)
E-mail: zmsu@nenu.edu.cn

[b] Dr. Y.-J. Tang, Prof. S.-L. Li, Prof. Y.-Q. Lan
Jiangsu Key Laboratory of Biofunctional Materials
School of Chemistry and Materials Science
Nanjing Normal University, Nanjing, 210023, Jiangsu (P.R. China)
E-mail: yqlan@njnu.edu.cn

Supporting information for this article is available on the WWW under <http://dx.doi.org/10.1002/chem.201500815>.

excellent work and have made a remarkable contribution to the study of removing organosulfur compounds by using MOFs.^[12] It ought to be an urgent issue to synthesize efficient storage materials that can enhance the adsorption and separation capacities of organosulfur compounds.

On the basis of the above, it is of great importance to design and synthesize MOFs that can have a high adsorption capacity for toxic phenyl compounds and can enhance the separation efficiency of organosulfur compounds simultaneously.

A large specific surface area, based on huge channels or large cages in the 3D structure, plays a central role in the efficient adsorption properties of MOFs.^[13] However, a framework with a large void space is generally susceptible to interpenetration, thus precluding high porosity. Therefore, how to overcome interpenetration is a key point in the synthesis of high porosity materials. One powerful strategy to design and construct non-interpenetrating structures is the use of mixed ligands to build porous MOFs, which not only have stable non-interpenetrating structures, but also possess relatively high surface areas.^[13b,14]

We have tried to add methyl groups and aromatic rings onto the inner surface of the pores to enhance the adsorption capacity of the toxic phenyl compounds. These functional groups may enhance the interactions between the host and guest and efficiently help to improve the adsorption abilities of these toxic compounds. Based on the structure–property insight mentioned above, we identified and synthesized four bidentate ligands H₂TDC (TDC = thieno[2,3-*b*]thiophene-2,5-dicarboxylate), H₂DMTDC (DMTDC = 3,4-dimethylthieno[2,3-*b*]thiophene-2,5-dicarboxylate), H₂MPTDC (MPTDC = 3-methyl-4-phenylthieno[2,3-*b*]thiophene-2,5-dicarboxylate), and H₂DPTDC (DPTDC = 3,4-diphenylthieno[2,3-*b*]thiophene-2,5-dicarboxylate) with different amounts of methyl and phenyl groups. We took advantage of the favorable constructional properties of these bidentate thiophene-containing ligands by combining them with a H₃BTB (BTB = benzene-1,3,5-tribenzoate) ligand and by using the solvothermal method, thus successfully designing and synthesizing a series of isorecticular MOFs (i.e., **NENU-511–NENU-514**; NENU = Northeast Normal University) with the same network topology. Nitrogen sorption isotherms indicate that these four compounds all have high surface areas. The benzene capacities of this **NENU** series are superior to those of the other MOF materials reported, and **NENU-513** has the highest capacity for benzene storage, thus demonstrating the benefits of introducing phenyl rings. This **NENU** series also has a higher adsorptive efficiency for the removal of organosulfur compounds than other MOFs in the ambient atmosphere. This type of material may be applied as an efficient adsorbent to the chemical industry in the future.

Results and Discussion

Heating a mixture of Zn(NO₃)₂·6H₂O, H₂TDC (H₂DMTDC, H₂MPTDC, or H₂DPTDC), and H₃BTB dissolved in *N,N*-diethylformamide (DEF) at 85 °C for 48 hours afforded pure-phase **NENU-511–NENU-514** as colorless crystals (the synthetic details

are given in the Supporting Information). Microscope pictures of **NENU-511–NENU-514** reveal that all of these four crystals have high crystallization qualities.

Single-crystal X-ray analysis reveals that **NENU-511** crystallizes in the tetragonal space group *P6₃/m*. The formula of **NENU-511** was determined as Zn₄O(TDC)(BTB)_{4/3} from a combination of elemental analysis and thermogravimetric analysis (TGA). Analysis of the structure reveals two different microporous cages (cages I and III; Figure 1 a) and one mesoporous cage (II; Figure 1 a) and one mesoporous

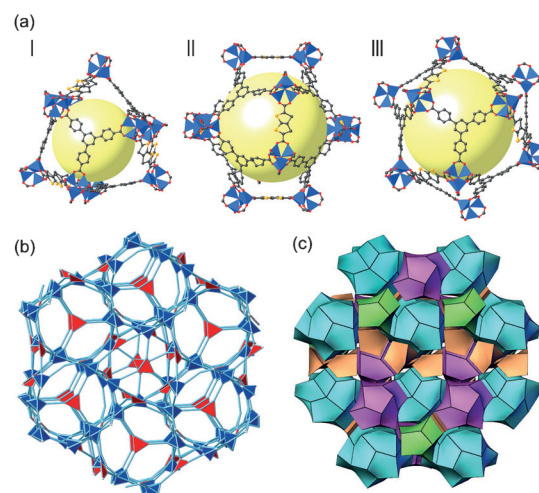


Figure 1. a) Microporous cages (I and III) and a mesoporous cage (II) in **NENU-511**. The big yellow ball is placed in the structure for clarity and to indicate space in the cage. Zn = blue tetrahedra; O = red balls; S = yellow balls; C = gray balls. Hydrogen atoms are omitted for clarity. b) The (3,6)-connected topology network in **NENU-511**. 3-connected nodes = red triangles; 6-connected nodes = blue octahedra. c) Natural tiling spaces of the **umt** topology.

cage (cage II; Figure 1 a). Each {Zn₄O(CO₂)₆} unit is connected by six BTB ligands to a six-connected node, and each BTB ligand connects three {Zn₄O(CO₂)₆} units, for which each carboxylic group binds to one {Zn₄O(CO₂)₆} unit. Such connectivity leads to a highly porous extended 3D framework with a typically 3D (3,6)-connected **umt** topology (Figure 1 b), which is isorecticular to **UMCM-2**. The use of PLATON/SQUEEZE showed that the accessible void in the desolvated structure of **NENU-511** corresponded to 82.42% of the total volume.

Due to the large pores in the structures and disorderly nature of the substituent groups, the crystal data of the **NENU-512–NENU-514** are not very good. However, powder X-ray diffraction (XRD) studies showed that **NENU-512–NENU-514** have adopted the same structural features of **NENU-511** and that all of the peaks match very well (Figure 2). This classic structure joins a select group of isorecticular frameworks that are tolerant to ligand substitution.

Framework **UMCM-1** has a similar structure to the frameworks in this **NENU** series. There are one type of microcage-like pore in **UMCM-1**, which is constructed from six BDC linkers, five BTB linkers, and nine {Zn₄O} clusters and one type of 1D *meso*-channel-like pore with an internal dimension of approximately 2.7 × 3.2 nm. In contrast to the pores constructed

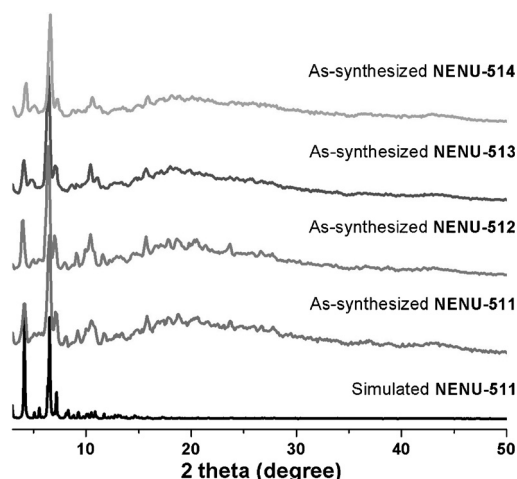


Figure 2. X-ray powder diffraction patterns of simulated **NENU-511** and as-synthesized **NENU-511–NENU-514**.

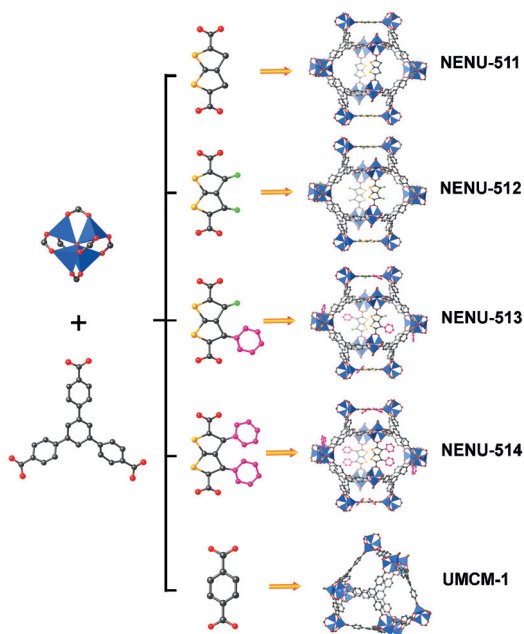


Figure 3. The $\{Zn_4O(CO_2)_6\}$ unit is connected with BTB and different TDC ligands to form MOFs. The cage(II) representations of **NENU-512–NENU-514** were simulated by using MaterialsStudio.^[15b] Zn: blue tetrahedrons; C: gray balls; O: red balls; S: yellow balls. The methyl and phenyl groups of the TDC ligand are highlighted in green and pink.

by H_2BDC ligands, the **NENU** series has new cage elements (Figure 3). To further determine the component of the structure, we used 1H NMR spectroscopic analysis to provide direct proof of the presence of the two organic ligands coordinated to the $\{Zn_4O\}$ clusters in **NENU-512–NENU-514**.^[15] 1H NMR spectroscopic measurements of acid-digested activated samples confirm the complete removal of the solvent molecules. Furthermore, the 1H NMR spectra of **NENU-512–NENU-514** show the presence of the two mixed ligands in different ratios. For example, the integral area of the H atoms in the 1H NMR spectrum of **NENU-512** shows the exact ratio of the two

ligands (H_2DMTDC/H_3BTB) to be 3:4, which is consistent with the real structure of **NENU-511**. To sum up, optical microscopy, powder XRD studies, and 1H NMR spectroscopic analysis of dissolved samples all indicate the isorecticular structure and the phase purity of these four materials (see the Supporting Information).

This high calculated porosity encouraged us to study the gas-sorption properties of the evacuated framework. The sample was fully activated by the synthetic procedure given in the Supporting Information, and the integrity of the framework was confirmed by powder X-ray diffraction (PXRD) studies (see Figure S2 in the Supporting Information). The N_2 -sorption isotherms of the **NENU** series show characteristic type-I behavior for microporous materials (see Figure S3 in the Supporting Information). Calculated from the nitrogen-adsorption data, the estimated BET surface areas of **NENU-511–NENU-514** are 4240, 3648, 3554, and 3457 m^2g^{-1} , respectively, and the corresponding Langmuir surface areas are 6491, 5640, 5438, and 5320 m^2g^{-1} , respectively. The porosity distribution, obtained by using the original density-functional theory method, showed a main narrow pore-width distribution in **NENU-511** of 14.8 Å, which is consistent with the single-crystal structure analysis. The pore-width distributions of the other three compounds are similar to that of **NENU-511**, with small differences owing to the existence of the methyl and phenyl groups on the ligands (see Figure S4 in the Supporting Information).

The H_2 -adsorption behaviors of these four compounds were also investigated (see Figure S5 in the Supporting Information). The corresponding H_2 -uptake capacities of **NENU-511–NENU-514** were 1.22, 1.30, 1.34, and 1.38 wt%, respectively, at 77 K and 1 bar. In terms of the **NENU** series, the H_2 -uptake capacity varied little, which is in contrast with the variation of the surface areas. According to previous reports, the H_2 -uptake capacity in the low-pressure region is mainly controlled by the hydrogen affinity toward the framework.^[16] Rather than large-sized pores, tiny pores (larger than the kinetic diameter of $H_2 = 2.89$ Å) are more favorable. So when the surface area decreases, the H_2 uptake of the **NENU** series increases.

The high porosity of the **NENU** frameworks allows potential access by a variety of organic vapor molecules, particularly the most common hydrocarbon benzene. The sorption behavior of benzene at 298 K is shown in Figure 4 and features typical type-I isotherms. The amounts adsorbed for benzene of **NENU-511–NENU-514** are 1556, 1519, 1687, and 1311 $mg g^{-1}$, respectively. To the best of our knowledge, the benzene capacities of **NENU-511–NENU-514** are superior to that of the other MOF materials (i.e., higher than **MOF-199** and the derivative compound **UMCM-1**,^[2] see the Supporting Information), especially for **NENU-513**, which has had the highest capacity in benzene storage up to now. The adsorption density of **NENU-513** achieved a level of 0.67 $g cm^{-3}$, which corresponds to 424 benzene molecules per unit cell at adsorption saturation. This value is very close to the density of liquid benzene (0.88 $g cm^{-3}$).

Careful analysis of these four adsorption curves showed that the benzene adsorption of **NENU-511** and **NENU-512** reach their saturation at $P/P_0 = 0.20$. In the structures of **NENU-511** and **NENU-512**, there are no special functional groups in the

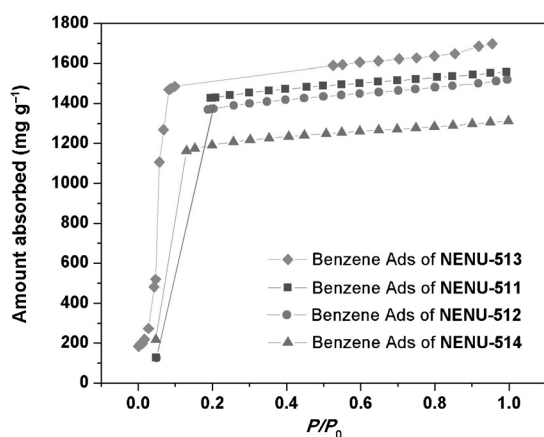


Figure 4. Benzene-adsorption isotherms for NENU-511–NENU-514 at 298 K.

pore. The high adsorption capacities of NENU-511 and NENU-512 can be generally ascribed to the large diameter of the pores in the structures, which are very spacious so that the pores can accommodate a large amount of benzene molecules; furthermore, the adsorption difference between NENU-511 and NENU-512 is mainly caused by the different sizes of their pores. On the other hand, the adsorption of benzene of NENU-513 and NENU-514 reach saturation earlier at $P/P_0 = 0.10$. The difference between these two types of saturation can be attributed to the existence of the phenyl rings on the inner surfaces of NENU-513 and NENU-514. There are a lot of phenyl rings in NENU-513 and NENU-514 that are raised on the inner surface of the pores; therefore, π - π^* stacking interactions between the benzene molecules and the host framework may help these guests to arrange themselves in an efficient way to favor the stacking configurations with the framework. Thanks to this strong interaction and relatively high porosity, NENU-513 has the highest benzene capacity of 1687 mg g^{-1} at 298 K. There are too many phenyl rings on the inner surface of NENU-514 relative to NENU-513, and the repulsion caused by steric effects weakens the π - π^* attractions; therefore, the adsorption property of NENU-514 is inferior relative to NENU-513. The combination of the effects caused by the reduction in porosity and the repulsion mentioned above results in an inferior adsorption capacity of NENU-514 relative to the other frameworks in the NENU series. In conclusion, we may suggest that the introduction of an appropriate amount of phenyl rings to the pore helped the formation of strong guest–host interactions between molecules and frameworks, thus resulting in the excellent benzene-adsorption performance of NENU-513.

Motivated by the permanent porosity and gas/solvent-sorption capabilities of the frameworks, NENU-511–NENU-514 were employed as adsorbents for desulfurization. We analyzed the adsorption capacities of the NENU series for 12 hours to calculate the adsorption efficiency. The adsorption experiments were carried out at 3500 ppmwS in isoctane for benzothio- phene (BT) and dibenzothio- phene (DBT), and all these four compounds exhibited relatively high capacities for the organo- sulfur compounds.

Frameworks NENU-511–NENU-514 exhibited tremendous capacities for BT and DBT: the BT capacities were 72, 45, 36, and 32 g S (kg MOF)^{-1} (1500 ppmwS), which are equivalent to 300, 189, 150, and 133 $\text{g BT (kg MOF)}^{-1}$ (1500 ppmwS), and the DBT capacities were 84, 69, 63, and 61 g S (kg MOF)^{-1} (1500 ppmwS), which were equivalent to 484, 395, 360, and 348 $\text{g DBT (kg MOF)}^{-1}$ (1500 ppmwS), respectively (Figure 5). As far as we

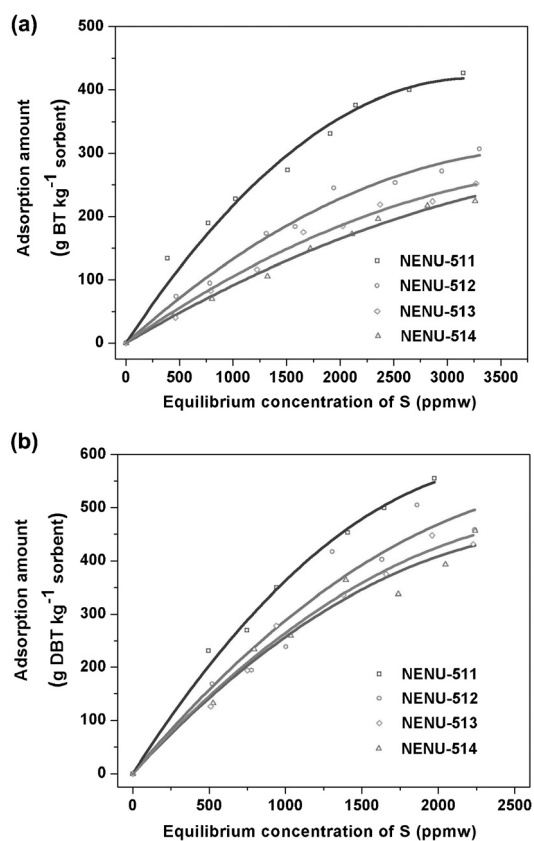


Figure 5. a) BT-adsorption isotherms for NENU-511–NENU-514 at 298 K from solutions in isoctane. b) DBT adsorption isotherms for NENU-511–NENU-514 at 298 K from solutions in isoctane.

know, the BT capacity of NENU-511 considerably exceeds that of other reported MOFs materials, and the DBT capacity of NENU-511 is close to that of the best-performing MOF known to date (i.e., UMCM-153 has a capacity of $89 \text{ g S (kg MOF)}^{-1}$; 1500 ppmwS) and superior to that of other MOF materials.^[17] Thus, each unit cell of NENU-511 can contain about 46.7 BT molecules or 54.8 DBT molecules at 1500 ppmwS.

The N_2 -sorption isotherms of BT@NENU-511, BT@NENU-512, BT@NENU-513, and BT@NENU-514 or DBT@NENU-511, DBT@NENU-512, DBT@NENU-513, and DBT@NENU-514 at 77 K show that the BET surface areas and Langmuir surface areas decreased after the adsorption of BT and DBT (Figure 6). This observation further proves that the BT or DBT molecules are trapped inside the pores of these compounds. The results obtained in this study are in good agreement with previous observations.

According to previous reports, the adsorption capacity in a given MOF may be determined by many factors, such as the

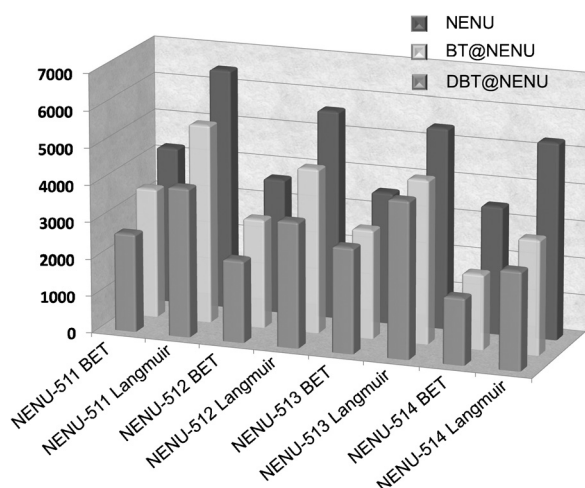


Figure 6. Schematic illustration that shows the comparison of the BET surface areas and Langmuir surface areas of the frameworks in the **NENU**, **BT@NENU**, and **DBT@NENU** series at different concentrations.

pore volume, pore shape, or the active sites on the inner surface of the pore. In the case of the **NENU** series, the most important factor is the spacious pores of the four compounds. Therefore, the amount of the organosulfur compounds adsorbed (BT or DBT) increases when the specific surface area of the compound becomes larger. In addition, the interactions between the aromatic linkers in the framework and conjugated organosulfur compounds may also play important roles in the adsorption process.^[18] There are four conjugated benzene rings in the ligand of H₃BTB, and these high atomic charges result in high aromatic interactions with the BT or DBT molecules. Furthermore, the thiophene rings on the inner surface may also have strong affinity to the same thiophene rings of the organosulfur compounds. In summary, the outstanding adsorption performances of this **NENU** series for BT and DBT may be attributed to a combination of the reasons mentioned above.

By comparing the adsorption capacity of the **NENU** series to the other classic MOFs previously reported, it is shown that **NENU-511** has the highest adsorptive efficiency for BT and the second highest adsorptive efficiency for DBT, which is only slightly less than **UMCM-153**. Thus, **NENU-511** is an excellent adsorbent for desulfurization.

Conclusion

We have successfully designed and synthesized a series of isorecticular MOFs **NENU-511–NENU-514** with the same network topology, by using the solvothermal reaction, and which all have high surface areas and strong adsorption capacities. Among these frameworks, **NENU-513** had a benzene capacity of 1687 mg g⁻¹, which is equivalent to 424 benzene molecules at 298 K. To the best of our knowledge, the benzene capacity of **NENU-513** ranks as the top among the MOF materials reported up to now, which demonstrates the benefits of introducing phenyl rings. With the permanent porosity obtained, the **NENU** series was used for adsorptive desulfurization, the results of which indicate that this **NENU** series has a higher ad-

sorptive efficiency in the removal of organosulfur compounds than other MOF materials, especially **NENU-511**, which has the highest adsorptive efficiency in the ambient atmosphere. This study has proven that the design and synthesis of targeted MOFs with higher surface areas and the presence of functional groups is an efficient method to enhance benzene storage capacity and the adsorption of organosulfur compounds. This synthetic strategy presents a progressive evolution for the construction of porous MOFs with mixed ligands, and functional applications of these MOFs in other adsorption fields are currently underway.^[19]

Acknowledgements

This work was financially supported by Pre-973 Program (No. 2010CB635114), the National Natural Science Foundation of China (No. 21371099 and 21471080), the Science and Technology Development Planning of Jilin Province (20140203006GX), the Jiangsu Specially Appointed Professor, the NSF of Jiangsu Province of China (No. BK20130043 and BK20141445), the Natural Science Research of Jiangsu Higher Education Institutions of China (No. 13KJB150021), the Priority Academic Program Development of Jiangsu Higher Education Institutions, and the Foundation of Jiangsu Collaborative Innovation Center of Biomedical Functional Materials.

Keywords: benzene storage · desulfurization · isostructural · metal–organic frameworks · phenyl groups

- [1] F. Stallmach, S. Gröger, V. Künzel, J. Kärger, O. M. Yaghi, M. Hesse, U. Müller, *Angew. Chem. Int. Ed.* **2006**, *45*, 2123–2126; *Angew. Chem.* **2006**, *118*, 2177–2181.
- [2] D. Britt, D. Tranchemontagne, O. M. Yaghi, *Proc. Natl. Acad. Sci. USA* **2008**, *105*, 11623–11627.
- [3] a) H. Wu, Q. Gong, D. H. Olson, J. Li, *Chem. Rev.* **2012**, *112*, 836–868; b) M.-H. Zeng, Y.-X. Tan, Y.-P. He, Z. Yin, Q. Chen, M. Kurmoo, *Inorg. Chem.* **2013**, *52*, 2353–2360.
- [4] a) J.-P. Zhang, X.-M. Chen, *J. Am. Chem. Soc.* **2008**, *130*, 6010–6017; b) J.-B. Lin, J.-P. Zhang, W.-X. Zhang, W. Xue, D.-X. Xue, X.-M. Chen, *Inorg. Chem.* **2009**, *48*, 6652–6660; c) Y.-X. Tan, Y.-P. He, J. Zhang, *ChemSusChem* **2012**, *5*, 1597–1601; d) Y.-X. Tan, Y.-P. He, J. Zhang, *Inorg. Chem.* **2012**, *51*, 9649–9654.
- [5] a) J.-R. Li, J. Sculley, H.-C. Zhou, *Chem. Rev.* **2012**, *112*, 869–932; b) L. E. Kreno, K. Leong, O. K. Farha, M. Allendorf, R. P. Van Duyne, J. T. Hupp, *Chem. Rev.* **2012**, *112*, 1105–1125; c) M. P. Suh, H. J. Park, T. K. Prasad, D.-W. Lim, *Chem. Rev.* **2012**, *112*, 782–835; d) H.-C. Zhou, J. R. Long, O. M. Yaghi, *Chem. Rev.* **2012**, *112*, 673–674; e) Y. Cui, Y. Yue, G. Qian, B. Chen, *Chem. Rev.* **2012**, *112*, 1126–1162; f) A. Bétard, R. A. Fischer, *Chem. Rev.* **2012**, *112*, 1055–1083.
- [6] a) E. D. Bloch, W. L. Queen, R. Krishna, J. M. Zadrozny, C. M. Brown, J. R. Long, *Science* **2012**, *335*, 1606–1610; b) Y.-Q. Lan, H.-L. Jiang, S.-L. Li, Q. Xu, *Adv. Mater.* **2011**, *23*, 5015–5020; c) J.-S. Qin, D.-Y. Du, W.-L. Li, J.-P. Zhang, S.-L. Li, Z.-M. Su, X.-L. Wang, Q. Xu, K.-Z. Shao, Y.-Q. Lan, *Chem. Sci.* **2012**, *3*, 2114–2118; d) W.-W. He, S.-L. Li, G.-S. Yang, Y.-Q. Lan, Z.-M. Su, Q. Fu, *Chem. Commun.* **2012**, *48*, 10001–10003; e) W.-W. He, S.-L. Li, W.-L. Li, J.-S. Li, G.-S. Yang, S.-R. Zhang, Y.-Q. Lan, P. Shen, Z.-M. Su, *J. Mater. Chem. A* **2013**, *1*, 11111–11116; f) W. Zhang, Y. Hu, J. Ge, H.-L. Jiang, S.-H. Yu, *J. Am. Chem. Soc.* **2014**, *136*, 16978–16981; g) Y. Hu, W. M. Verdegaal, S.-H. Yu, H.-L. Jiang, *ChemSusChem* **2014**, *7*, 734–737; h) Z.-R. Jiang, H. Wang, Y. Hu, J. Lu, H.-L. Jiang, *ChemSusChem* **2015**, *8*, 878–885.
- [7] a) X. Lin, A. J. Blake, C. Wilson, X. Z. Sun, N. R. Champness, M. W. George, P. Hubberstey, R. Mokaya, M. Schröder, *J. Am. Chem. Soc.* **2006**, *128*,

- 10745–10753; b) L. Hou, Y.-Y. Lin, X.-M. Chen, *Inorg. Chem.* **2008**, *47*, 1346–1351; c) C. Yang, U. Kaipa, Q. Z. Mather, X. Wang, V. Nesterov, A. F. Venero, M. A. Omary, *J. Am. Chem. Soc.* **2011**, *133*, 18094–18097; d) S. Amirjalayer, R. Schmid, *J. Phys. Chem. C* **2012**, *116*, 15369–15377; e) N. A. Ramsahye, P. Trens, C. Shepherd, P. Gonzalez, T. K. Trung, F. Ragon, C. Serre, *Microporous Mesoporous Mater.* **2014**, *189*, 222–231.
- [8] V. Chandra Srivastava, *RSC Adv.* **2012**, *2*, 759–783.
- [9] a) H. Zhang, J. Gao, H. Meng, C.-X. Li, *Ind. Eng. Chem. Res.* **2012**, *51*, 6658–6665; b) J. Xu, S. Zhao, W. Chen, M. Wang, Y.-F. Song, *Chem. Eur. J.* **2012**, *18*, 4775–4781.
- [10] K. A. Cychoz, R. Ahmad, A. J. Matzger, *Chem. Sci.* **2010**, *1*, 293–302.
- [11] a) K. A. Cychoz, A. G. Wong-Foy, A. J. Matzger, *J. Am. Chem. Soc.* **2008**, *130*, 6938–6939; b) K. A. Cychoz, A. G. Wong-Foy, A. J. Matzger, *J. Am. Chem. Soc.* **2009**, *131*, 14538–14543.
- [12] a) T.-H. Park, K. A. Cychoz, A. G. Wong-Foy, A. Dailly, A. J. Matzger, *Chem. Commun.* **2011**, *47*, 1452–1454; b) N. A. Khan, S. H. Jhung, *Angew. Chem. Int. Ed.* **2012**, *51*, 1198–1201; *Angew. Chem.* **2012**, *124*, 1224–1227; c) N. A. Khan, J. W. Jun, J. H. Jeong, S. H. Jhung, *Chem. Commun.* **2011**, *47*, 1306–1308.
- [13] a) K. Koh, A. G. Wong-Foy, A. J. Matzger, *J. Am. Chem. Soc.* **2009**, *131*, 4184–4185; b) K. Koh, A. G. Wong-Foy, A. J. Matzger, *Angew. Chem. Int. Ed.* **2008**, *47*, 677–680; *Angew. Chem.* **2008**, *120*, 689–692.
- [14] a) H. Furukawa, N. Ko, Y. B. Go, N. Aratani, S. B. Choi, E. Choi, A. O. Yazaydin, R. Q. Snurr, M. O’Keeffe, J. Kim, O. M. Yaghi, *Science* **2010**, *329*, 424–428; b) Y.-B. Zhang, W.-X. Zhang, F.-Y. Feng, J.-P. Zhang, X.-M. Chen, *Angew. Chem. Int. Ed.* **2009**, *48*, 5287–5290; *Angew. Chem.* **2009**, *121*, 5391–5394.
- [15] a) L. Liu, K. Konstas, M. R. Hill, S. G. Telfer, *J. Am. Chem. Soc.* **2013**, *135*, 17731–17734; b) San Diego, CA: Accelrys Inc. (**2009**).
- [16] a) M. Dincă, A. Dailly, Y. Liu, C. M. Brown, D. A. Neumann, J. R. Long, *J. Am. Chem. Soc.* **2006**, *128*, 16876–16883; b) M. Dincă, J. R. Long, *Angew. Chem. Int. Ed.* **2008**, *47*, 6766–6779; *Angew. Chem.* **2008**, *120*, 6870–6884; c) S. Yang, X. Lin, A. Dailly, A. J. Blake, P. Hubberstey, N. R. Champness, M. Schröder, *Chem. Eur. J.* **2009**, *15*, 4829–4835; d) L. J. Murray, M. Dinca, J. R. Long, *Chem. Soc. Rev.* **2009**, *38*, 1294–1314; e) J. Sculley, D. Yuan, H.-C. Zhou, *Energy Environ. Sci.* **2011**, *4*, 2721–2735.
- [17] J. K. Schnobrich, O. Lebel, K. A. Cychoz, A. Dailly, A. G. Wong-Foy, A. J. Matzger, *J. Am. Chem. Soc.* **2010**, *132*, 13941–13948.
- [18] S.-L. Li, Y.-Q. Lan, H. Sakurai, Q. Xu, *Chem. Eur. J.* **2012**, *18*, 16302–16309.
- [19] The Supporting Information includes the experimental details, N₂- and H₂-adsorption data, PXRD patterns, TGA, IR spectroscopic data, and additional figures for the **NENU** series. CCDC 102453 (**NENU-511**) contains the supplementary crystallographic data for this paper. These data are provided free of charge by The Cambridge Crystallographic Data Centre.

Received: February 27, 2015

Published online on May 26, 2015